SUPPORTING INFORMATION

Table of Contents

1. Extended experimental procedures 1
Bacterial strains and general growth conditions 1
Genomic modification of **Porphyromonas gingivalis** 1
Subcellular fractionation of **P. gingivalis** *cells* 2
Processing of proRgpB by intact bacterial cells and cell extracts 2
Western-blot analyses 2
Proteolytic activity assays 2
Expression and purification of recombinant PorU 2
Flow cytometry 3
In vitro *selection of anti-PorU aptamers and testing* 3
Labelling of rPorU with biotinylated chloromethylketones 4
Multi-angle laser light scattering after size-exclusion chromatography 4
Crystallization and diffraction data collection 4
Structure solution and refinement 4
Homology modelling of competent PorU 5
Miscellaneous 5
2. Supplementary figures 6
Supplementary Figure 1 6
Supplementary Figure 2 7
Supplementary Figure 3 8
Supplementary Figure 4 9
Supplementary Figure 5 10
Supplementary Figure 6 11
Supplementary Figure 7 12
3. Supplementary tables 13
Supplementary Table 1 13
Supplementary Table 2 14
Supplementary Table 3 15

4. Supplementary references 16

---

1. EXTENDED EXPERIMENTAL PROCEDURES

Bacterial strains and general growth conditions — *P. gingivalis* wild-type strain W83 and variants were grown in enriched trypticase soy broth (eTSB; 30 g/L) supplemented with yeast extract (5 g/L), L-cysteine (0.5 g/L), menadione (2 mg/L) and hemin (5 mg/L). Plated eTSB was further supplemented with 5% defibrinated sheep blood and 1,5% agar. Cultures were incubated at 37ºC in an anaerobic chamber (Don Whitley Scientific, UK) with an atmosphere of 85% nitrogen, 5% hydrogen, and 10% carbon dioxide. *Escherichia coli* strain DH5α grown in Luria-Bertani medium (LB; Lennox) was used for plasmid replication. Antibiotic selection was performed with erythromycin (5 μg/mL) and ampicillin (100 μg/mL) for *P. gingivalis* and *E. coli*, respectively.

***Genomic modification of* P. gingivalis —** Generation of *P. gingivalis* PorU point mutants was performed by homologous recombination with suicide plasmids derived from master plasmid pPorU-E, which was subjected to PCR-based mutagenesis with the SLIM methodology (1) to introduce a C-terminal His_8-tag,

giving rise to plasmid pPorUHis (Suppl. Table 2). Primer sequences used are listed in Suppl. Table 3. In subsequent reactions, mutations were introduced into pPorUHis following either the SLIM methodology (mutants PorU-627-632sGG, PorU-C^{690}A, PorU-R^{722}A, and PorU-627-632sGG), Gibson cloning (PorU-850-868sGAGA; (2)), or phosphorylated PCR-product cyclisation (PorU-H^{657}A). Deletion of the *sov* gene was performed with the suicide plasmid pUSovAtB generated from the pUC19. Briefly, DNA fragments flanking the *sov* gene were amplified from genomic DNA. The upstream and the downstream fragment were amplified with primers SovUpF plus SovUpR and SovDwR plus SovDwR, respectively. The tetracycline cassette was amplified from the p6HRgpBt-A (3) plasmid with primers SovTetF and SovTetR. All four elements of pUSovAtB were combined by ligation of PCR fragments digested by restriction enzymes. Removal of the *rgpB* gene was performed with modified plasmid p6HRgpBt-A by deleting most of the coding sequence in a single PCR reaction followed by Gibson cloning. This gave rise to plasmid p6HRgpBt-A-d410. All new plasmids were verified by sequencing and introduced for recombination into the *P. gingivalis* W83 wild type by electroporation as described (3). Erythromycin at 5 μg/mL or teteracycline at 1 μg/mL were used for recombinant clone selection. All mutants were confirmed by partial sequencing of the respective genomic DNA.

***Subcellular fractionation of* P. gingivalis *cells* —** Stationary cell cultures of wild-type and mutant strains were adjusted to OD_{600}=1.5 with fresh eTSB supplemented with 2 mM 2,2'-dithiodipyridine and incubated for 15 min prior to centrifugation (5,000×*g*; 20 min). The resulting cell-free culture medium was designated the 'supernatant fraction' (S). Cells were then collected, washed and resuspended in ice-cold phosphate-buffered saline (PBS) supplemented with cOmplete EDTA-free inhibitor mix (Roche) plus 0.2 mM of tosyl-L-lysyl-chloromethane hydrochloride (TLCK) (Sigma), disrupted with a Constant System cell disruptor (BT40/TS2/AA, Thermo scientific) operating at 30 kPa, and digested with DNase I (Roche) at 0.02 mg/mL. After 30 min of incubation on ice, the 'cell extract' (CE) fraction was collected and the remaining solution was ultracentrifuged at 150,000×*g* for 1 h to separate the 'periplasmic/cytoplasmic' fraction (PC) from the insoluble membrane fraction. Next, 200 mM magnesium chloride, 10% Triton x100 was added to the membrane pellet for 30 min at 4°C to dissolve inner membrane components. After further centrifugation at 150,000×*g* for 1 h, the insoluble fraction was resuspended by sonication in PBS supplemented with inhibitors and designated the 'outer membrane' fraction (OM). Protein concentrations of each fraction were determined using the BCA Protein Assay Kit (Thermo Scientific) using bovine serum albumin (BSA; Sigma Aldrich) as a standard, and 5 mM TLCK was added to all fractions prior to storage at -20°C.

Processing of proRgpB by intact bacterial cells and cell extracts — Pro-RgpB-C_{449}A-H6 bearing a C-terminal His_6-tag and mature wild-type RgpB-H6 were purified as described before (5, 6). *P. gingivalis* cells were cultivated until reaching the early stationary phase and adjusted to OD_{600}≈1 before pelleting (5,000×*g*; 10 min). Cells were washed and diluted with PBS. For experiments with separate cell fractions, bacteria were sonicated (10 pulses à 5s; 14 W per pulse) to obtain the cell lysate, and then centrifuged (150,000×g; 1 h) to obtain the PC fraction. ProRgpB-C_{449}A-H6 (0.05 mg/mL) was then incubated at room temperature in assay buffer supplemented with 5 mM dithiothreitol (DTT) in the presence of either full bacterial suspension or the PC fraction at a 1:4 ratio (v/v; equivalent to OD_{600}≈0.25). At various time points, aliquots containing 0.1 μg of progingipain were taken, and the reaction was stopped at 100°C with reducing sample buffer. Maturation of progingipain was followed by western blot using polyclonal antibodies (pAb) anti-RgpB and anti-HisTag, and the monoclonal antibody (mAb) anti-CTD (for the detection of the CTD of RgpB). Mature RgpB-H6 was used as control.

Western-blot analyses — Samples of the distinct subcellular fractions were analysed by SDS-PAGE and blotted on nitrocellulose membranes. Ponceau S staining was employed to visualise transferred proteins. After extensive washing with water to remove the stain, membranes were blocked at 20ºC for 2 h in 5 % non-fat skim milk in PBS with 0.05% [v/v] Tween-20 (PBS-T) and subsequently incubated overnight at 4 °C with the following primary antibodies diluted in PBS-T with 5% milk: mAb 7G9 (for the detection of PorU), pAb GP-1 (for the detection of RgpB), and anti-CTD. Next, blots were incubated for 1 h at room temperature with goat anti-mouse horseradish peroxidase-conjugated IgG (for anti-PorU blots) or anti-rabbit horseradish peroxidase-conjugated secondary antibodies (for anti-RgpB and anti-CTD blots), both at 1:20,000 dilution.

Proteolytic activity assays — Proteolytic activity of gingipains Kgp and RgpA/B in the extracellular milieu were analysed in a SpectroMax M5 microplate reader (Molecular Devices) by following the increase of absorbance at λ=405 nm caused by cleavage of the chromogenic substrates AcO-K-*p*-nitroanillide and PheCO-R-*p*-nitroanillide, respectively, as described (4). Each experiment was performed in triplicate and the activity was given as percentage of the wild-type activity.

Expression and purification of recombinant PorU — Genomic DNA was isolated from wild-type *P. gingivalis* strain W83 using the Genomic Mini System (A&A Biotechnology, Gdansk, Poland), according to

the manufacturer's instructions. A fragment encoding residues Q^{24}-Q^{1158}, thus lacking the predicted signal peptide (M^{1}-A^{23}), was amplified by PCR, purified, and cloned into the pETDuet-1 expression vector using *Pst*I/*Xho*I restriction enzymes and primers listed in Suppl. Table 3. The resulting plasmid, pET-Duet-1-PorU, was verified by DNA sequencing. The construct encoded an N-terminal His_6-tag, a linker, and the cloned protein, thus spanning the sequence M^{-22}GSSHHHHHHSQDPNSSSARLQ^{-1}+Q^{24}–Q^{1158}, hereafter rPorU.

Expression plasmids were transformed into the *Escherichia coli* strain BL21 (DE3) strain under the control of the T7 promoter. Transformed cells were grown in LB with ampicillin (100 μg/mL) at 37°C until OD_{600}≈0.2-0.3, and then for a further 30 min at 20°C. Protein expression was induced with 0.2 mM isopropyl-1-thio-β-*D*-galactopyranoside and allowed to proceed for 16 h at 20ºC. Thereafter, cells were harvested by centrifugation (15 min, 5000×*g*, 4°C), resuspended in 40 mM imidazole pH 7.4, 20 mM trisodium phosphate, 0.5 M sodium chloride, 0.02% sodium azide and then lysed by sonication using a Branson Digital 450 sonifier (Branson Ultrasonics, Danburry, CT). The cell lysate was clarified by ultracentrifugation (40 min, 40,000×*g*, 4°C), filtrated through a 0.45-μm syringe filter and purified by nickel nitrilotriacetic acid affinity chromatography (Ni-NTA) using a column with 10 mL pre-equilibrated Nickel Sepharose 6 Fast Flow resin (GE Healthcare Life Sciences) at 4°C. The rPorU protein was eluted with 20 mM trisodium phosphate pH 7.4, 0.5 M sodium chloride, 250 mM imidazole, 0.02% sodium azide. Protein-containing fractions were pooled, concentrated, and further purified by size-exclusion chromatography (SEC) at a flow rate of 1.5 mL/min in a HiLoad 16/600 Superdex 200 pg column (GE Healthcare) attached to an ÄKTA Pure FPLC system (GE Healthcare) and equilibrated with 5 mM Tris·HCl pH 8.0, 50 mM sodium chloride, 0.02% sodium azide. The elution profile was monitored by measuring A_{280}, and 1 mL fractions containing the protein were collected, dialysed overnight against 20 mM Tris·HCl pH 7.5, 20 mM sodium chloride and further purified by ionic-exchange chromatography in a TSKgel DEAE-2SW column (TOSOH Bioscience) equilibrated with the latter buffer. A gradient of 5-to-70% 20 mM Tris·HCl pH 7.5, 0.5 M sodium chloride was applied over 30 mL, and samples were collected and pooled. Subsequently, each pool was concentrated by ultrafiltration and subjected to a final SEC step in a Superdex 200 10/300 column (GE Healthcare Life Sciences) in 20 mM Tris·HCl pH 7.5, 150 mM sodium chloride. The protein concentration was estimated by measuring A_{280} in a spectrophotometer (NanoDrop; ThermoFisher Scientific) and applying the respective theoretical extinction coefficient (1.01 for rPorU) as calculated by *ProtParam* (http://web.expasy.org). Concentrations were also measured with the BCA Protein Assay Kit as aforementioned. A selenomethione variant of rPorU was obtained in an equivalent way, except that selenomethionine was used instead of methionine in the cell culture medium.

Flow cytometry — *P. gingivalis* W83 strains producing PorUHis and its variants were grown in eTSB until they reached the late exponential stationary growth phase (OD_{600}≈1.2–1.5). Bacterial cells were harvested by centrifugation, washed twice with PBS, and adjusted to OD_{600}≈1.0 with staining buffer comprising PBS supplemented with 0.2% BSA, cOmplete EDTA-free inhibitor mix (Roche), and 1 mM tosyl-L-lysyl-chloromethane hydrochloride (Sigma Aldrich). Then, 150 μL cell suspension was transferred to a 96-well conical plate, and cells were collected by centrifugation (5 min, 1000×g). The resulting pellets were resuspended in staining buffer containing the 7G9 mAb at 40 μg/mL total protein concentration and incubated for 30 min. Thereafter, cells were washed twice with PBS and centrifuged (5 min, 1000×g). The new pellet was resuspended in staining buffer containing goat anti-mouse antibody conjugated with Alexa Fluor 488 (Life Technologies) at 1:150 dilution and incubated for 30 min. Cells were washed twice with PBS and transferred to specific tubes for fluorescence-activated cell sorting (FACS). After staining, one-color flow cytometry analyses were performed using a FACSCalibur apparatus (BD Biosciences) operating with the *CellQuest* software (BD Biosciences). Graphs were prepared using the *FlowJo* program (Ashland, USA).

In vitro *selection of anti-PorU aptamers and testing* — Aptamers recognising the rPorU protein were selected from a ssDNA library by the SELEX method according to (8). Shortly, a library of polynucleotides containing a 40-nt random sequence flanked by conserved sequences for PCR amplification (5′-CATGCTTCCCCAGGGAGATG-N_{40}-GAGGAACATGCGTCGCAAAC-3′) was selected with rPorU immobilised on magnetic beads (tosyl-activated Dynabeads M-280; Thermo Scientific) in binding buffer (PBS plus 5 mM magnesium chloride, 10 mM potassium chloride, 0.01% Tween, and tRNA and BSA as competitors). In every cycle, the ssDNA pool captured by the rPorU-beads was amplified by PCR using universal primers and ssDNA was restored by lambda exonuclease treatment. Eleven cycles of SELEX were performed with increasing selective pressure. The final aptamer pool was cloned into the pTZ57R/T vector and sequenced. From the most abundant sequences, six representatives were chosen for subsequent assays. Aptamers were carbofluorescein-labeled at the 5' end and used for K_d determination through thermoforesis according to (9). Their ability to inhibit PorU activity *in vivo* was tested on *P. gingivalis* liquid cultures at mid-exponential phase. Cells were rinsed with PBS and pretreated with 1 μM of the specific Rgp inhibitor KYT-1 (5) for 10 min at 37ºC. After centrifugation, cells were resuspended in fresh culture medium and aptamers

were added at 10 μM concentration. Rgp activity was determined using benzoyl-L-arginine-*p*-nitroanilide (BA*p*NA) (Sigma Aldrich) as substrate according to (10).

Labelling of rPorU with biotinylated chloromethylketones — rPorU was expressed and purified as described above but SEC was performed immediately after Ni-NTA chromatography to reduce rPorU dimer formation. The buffer 10 mM HEPES pH 7.5, 100 mM sodium chloride was used for the SEC step. Labelling was performed in reaction buffer comprising 20 mM Bis-Tris pH 6.5, 150 mM sodium chloride, 5 mM calcium chloride, 0.02% sodium azide. Fractions of 1 μg of rPorU corresponding to the different oligomeric states (aggregate, 408 kDa, 255 kDa, 162 kDa, and 51 kDa) were incubated in reaction buffer containing freshly prepared 20 mM L-cysteine for 15 min at 37°C. Then, biotinylated phenylalanylprolinylargininyl chloromethylketone (Biot-F-P-R-ck; Bachem) was added to 5 μM final concentration, and the mixture was incubated for 15 min at 37°C. Samples were boiled with sample buffer containing 50 mM dithiothreitol, separated by SDS-PAGE (Novex system), electro-transferred to nitrocellulose membranes, and blocked with 5% BSA in Tween-Tris-buffered saline (TTBS; 20 mM Tris·HCl, 0.5 M sodium chloride, 0.1% Tween-20, pH 7.5) overnight at 4°C. Membranes were washed five times with TTBS, incubated with Streptavidin−Peroxidase Polymer (Sigma Aldrich) at 1:20,000 in TTBS containing 5% BSA for 60 min at room temperature, and developed using a TMB Membrane Peroxidase Substrate System (BD Biosciences) according to the manufacturer's instructions.

Multi-angle laser light scattering after size-exclusion chromatography — To determine the actual molecular mass of full-length rPorU, multi-angle laser light scattering (SEC-MALLS) was performed in a Dawn Helios II apparatus (Wyatt Technologies) coupled to a SEC Superdex 200 10/300 Increase column as previously reported (6, 7). The later column was equilibrated with 20 mM Tris·HCl pH 7.4, 150 mM sodium chloride at 25ºC and operated at a flow rate of 0.5 mL/min at the joint IBMB/IRB Automated Crystallography Platform (PAC; www.ibmb.csic.es/en/facilities/automated-crystallographic-platform) at Barcelona Science Park (Catalonia, Spain). A total volume of 60 mL of protein solution at 1.2 mg/mL was employed. *Astra 7* software (Wyatt Technologies) was used for data processing and analysis, for which a typical dn/dc value for proteins (0.185 mL/g) was assumed. All experiments were performed in triplicate.

Crystallization and diffraction data collection — Crystallization assays were performed by the sitting-drop vapor diffusion method. Reservoir solutions were prepared by a Tecan robot and 100-nL drops were dispensed on 96-well 2-drop Swissci PS MRC plates (Molecular Dimensions) by a Phoenix nanodrop robot (Art Robbins) or a Cartesian Microsys 4000 XL robot (Genomic Solutions) at PAC. Plates were stored in Bruker steady-temperature crystal farms at 4°C or 20ºC. Successful conditions were scaled up to the microliter range in 24-well Cryschem crystallisation dishes (Hampton Research).

The best crystals of full-length native and selenomethionine-derivatized rPorU were obtained at 20ºC in drops with 1 μL of protein solution (at 5-10 mg/mL in 20 mM Tris·HCl pH 7.5, 150 mM sodium chloride) and 1 μL of reservoir solution (100 mM HEPES pH 7.5, 200 mM calcium chloride, 28-32% [v/v] polyethylene glycol 600). Crystals were cryoprotected by rapid passage through drops containing increasing amounts of glycerol (5-to-20%; v/v). Complete datasets were collected at 100 K from liquid-nitrogen flash-cryocooled crystals (Oxford Cryosystems 700 series cryostream) at the ESRF synchrotron (Grenoble, France) and the ALBA synchrotron (Cerdanyola, Catalonia/Spain) using Pilatus 6M detectors. Crystals were hexagonal and contained two protein molecules in the asymmetric unit (solvent content 66%, V_M=3.7Å^3/Da; (8)). Diffraction data were processed with programs *Xds* (9) and *Xscale*, and transformed with *Xdsconv* to MTZ-format suitable for the *Phenix* (10) and *CCP4* (11) suites of programs. Suppl. Table 1 provides essential statistics on data processing.

Structure solution and refinement — The structure of full-length rPorU was solved by single-wavelength anomalous diffraction with data collected at the selenium absorption peak wavelength from a selenomethionine-derivatised crystal. Data processed with separate Friedel mates served to identify 57 out of the 64 expectable selenium sites based on anomalous differences with program *Shelxd* (12). Subsequent phasing with *Shelxe* (13), which applied the free-lunch algorithm, identified the correct hand based on the pseudo-free correlation coefficient (56% *vs.* 34%), and produced initial phases with an estimated mean figure-of-merit of 51%. However, both the autotracing procedure of *Shelxe* and the *Autobuild* protocols from the *Phenix* package (14, 15) yielded only very partial and fragmented models. Thereafter, many rounds of manual model building with the *Coot* program (16), which were assisted by homology models and the positions of the selenomethionine residues, alternated with crystallographic refinement with the *Refine* protocol of *Phenix* (17) and with the *Buster* (18) program, which included non-crystallographic symmetry restraints and translation/libration/screw-motion refinement, until the final model was obtained. The latter included residues Q^{24}-Q^{1158} from molecules A and B except for three loops of the catalytic domain (V^{622}-A^{637}, D^{691}/T^{689}-G^{703}/A^{702} and A^{589}/C^{586}-I^{613}). In molecule B, six residues from the N-terminal tag (S^{-6}-Q^{-1}) could be traced preceding

Q^{24}. One structural calcium ion was found in each of the CBML2 (calcium site 1) and IGL2 (calcium site 2) domains. Calcium sites 1 included two solvent molecules each. Given the resolution of the final Fourier maps, no attempt was undertaken to model further solvent molecules or ligands.

Model completion and refinement was very laborious, greatly hampered by the low resolution (3.35Å), high Wilson B-factor (107 $Å^2$) and anisotropy (variation of 31 $Å^2$ in the principal components) of the diffraction data. In addition, the structure was highly flexible (average thermal displacement parameter≈140 $Å^2$) due to small crystal-contact and interdomain interfaces, and to partial disorder of the catalytic domain, for which only the NTS-CD (I^{405}-A^{588} and I^{405}-A^{585} in molecules A and B, respectively) could be continuously traced. From the CTS-CD, segments M^{614}-D^{621}, K^{638}-C^{690} and E^{704}-L^{789} (molecule A) and M^{614}-D^{621}, K^{638}-A^{688} and G^{703}-L^{789} (molecule B) were tentatively built and assigned to sequence, partially assisted by secondary structure predictions. Generally, 58 and 85 residues were truncated for their side chains after the respective Cβ atoms in molecules A and B, respectively. In addition, the last three domains of molecule B were poorly defined in the Fourier maps. Overall, this caused molecule A to be better defined than molecule B (average thermal displacement parameters of 134 $Å^2$ *vs.* 147 $Å^2$). Despite all these handicaps, the agreement between observed and calculated structure-factor amplitudes was very good (0.94) and the overall quality of the model notable, as revealed by the final refinement and model quality statistics reported in Suppl. Table 1. The final structure of full-length dimeric rPorU was validated with the *wwPDB Validation Service* at https://validate-rcsb-1.wwpdb.org/validservice and deposited with the PDB at www.pdb.org (access code 6ZA2).

Homology modelling of competent PorU — A homology model for the competent CD (residues I^{405}-L^{789}) of PorU was computed automatically with *Raptor-X* (http://raptorx.uchicago.edu/StructurePrediction/predict; (19)), which uses profile-entropy scoring, multiple-template threading, and conditional random fields to integrate a variety of biological signals in a non-linear threading score function to produce high-quality models, even for targets with only remote templates. These calculations identified *P. gingivalis* RgpB (PDB 1CVR, 4IEF; (20, 21)) as the closest structural relative and template for comparative modelling with *Modeller* (22). Superposition onto the equivalent domain of the crystal structure revealed a very good match for segments I^{405}-D^{575} and T^{751}-L^{789} except for some loops. Thus, a model was constructed by assembling these segments, as well as the upstream and downstream domains, from the experimental structure and the intervening region R^{576}-R^{750} from the homology model. A substrate pentapeptide encompassing the sequence from RgpB recognized by PorU (E-G-T✂S-I) was modelled based on the superposed coordinates of Kgp in complex with the KYT-36 inhibitor (PDB 6I9A; (23)). The homology model was visually inspected and corrected for minor intra- and interdomain clashes and subjected to geometric refinement with *Coot* and the *Geometry_minimization* routine of *Phenix*. Thereafter, the CTD was rotated outward by 90º around G^{1052} with *Coot* and the geometry of the flanking residues was refined with the 'regularize zone' option of the program. The final comparative model for active monomeric *P. gingivalis* PorU was validated with *Molprobity* (24) at molprobity.biochem.duke.edu: poor rotamers, 107 (11.4%); Ramachandran outliers/favoured/all residues, 3(0.3%)/1075(94.6%)/1136(100%); Cβ deviations, 0; residues with poor bonds/angles, 0/7; *rmsd* bonds/angles, 0.003 Å/0.86º; all-atom clash-score, 2.03 (99^{th} percentile); *Molprobity* score: 2.14 (68^{th} percentile). This model can be downloaded as part of the supplementary material.

Miscellaneous — Structural similarity searches were performed with *Dali* (25) and *PDBeFOLD* at pdbe.org/fold based on program *SSM* (26). Figures were prepared with the *Chimera* program (27). Secondary structure predictions were performed with *Jpred4* (28). Protein interfaces were calculated with *PDBePISA* (29) at www.ebi.ac.uk/pdbe/pisa. The interacting surface of a complex was defined as half the sum of the buried surface areas of either molecule.

2. SUPPLEMENTARY FIGURES

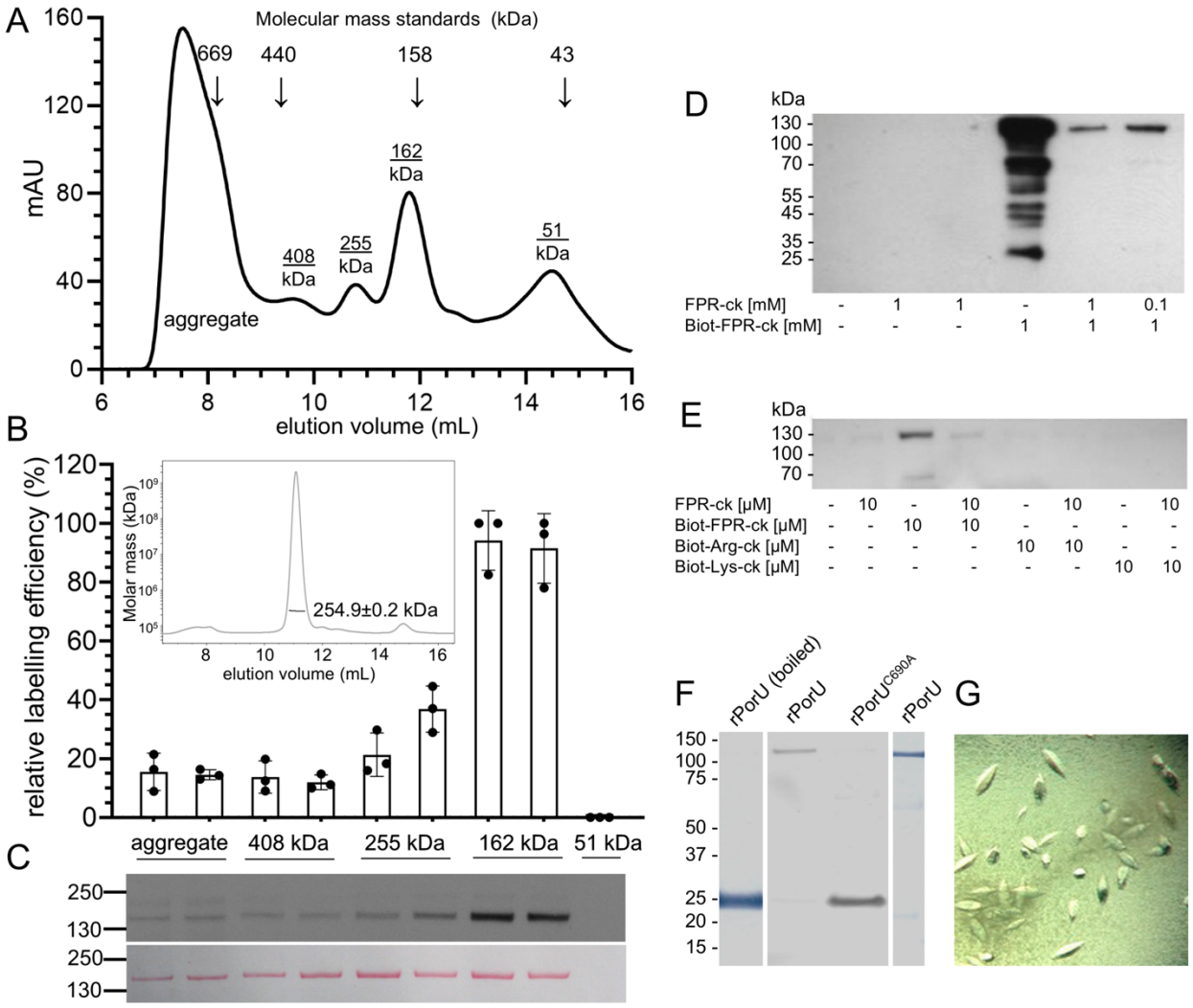

***Suppl. Figure 1* — Analysis of rPorU oligomerisation states and crystallisation. (A)** Calibrated size-exclusion chromatography profile showing different oligomeric states of rPorU, with thyroglobulin (669 kDa), ferritin (440 kDa), aldolase (158 kDa), and ovalbumin (43 kDa) as molecular-mass markers. **(B)** Labelling efficiency of rPorU oligomeric states with Biot-F-P-R-ck determined by SDS-PAGE densitometry. Each peak contains a left and a right fraction corresponding to the ascending and descending shoulders of the peak, respectively. Dots depict the individual measurements (n=3, mean±SD). The inset shows the SEC-MALLS analysis of purified rPorU (injected at 1.2 mg/mL), which reveals a molecular mass consistent with a dimer (~255 kDa). **(C)** One of the three SDS-PAGE gels used for the densitometry in (B) is shown in the upper panel together with the loading control (Ponceau Red) in the lower panel. **(D)** Western blotting analysis of Biot-F–P–R-ck labelling of monomeric rPorU, with or without previous treatment with the non-biotinylated reagent. **(E)** Similar experiment to (D) further showing the lack of effect when using Biot-R-ck and Biot-K-ck. **(F)** Same as (D) for boiled rPorU and the $C^{690}A$ mutant whose full-length forms are not labelled. Instead, a non-specific biotinylated 25-kDa fragment, apparently possessing a nucleophilic group reactive with chloromethyl ketones, was observed. **(G)** Hexagonal crystals of wild-type rPorU from *P. gingivalis* were used for structural analysis.

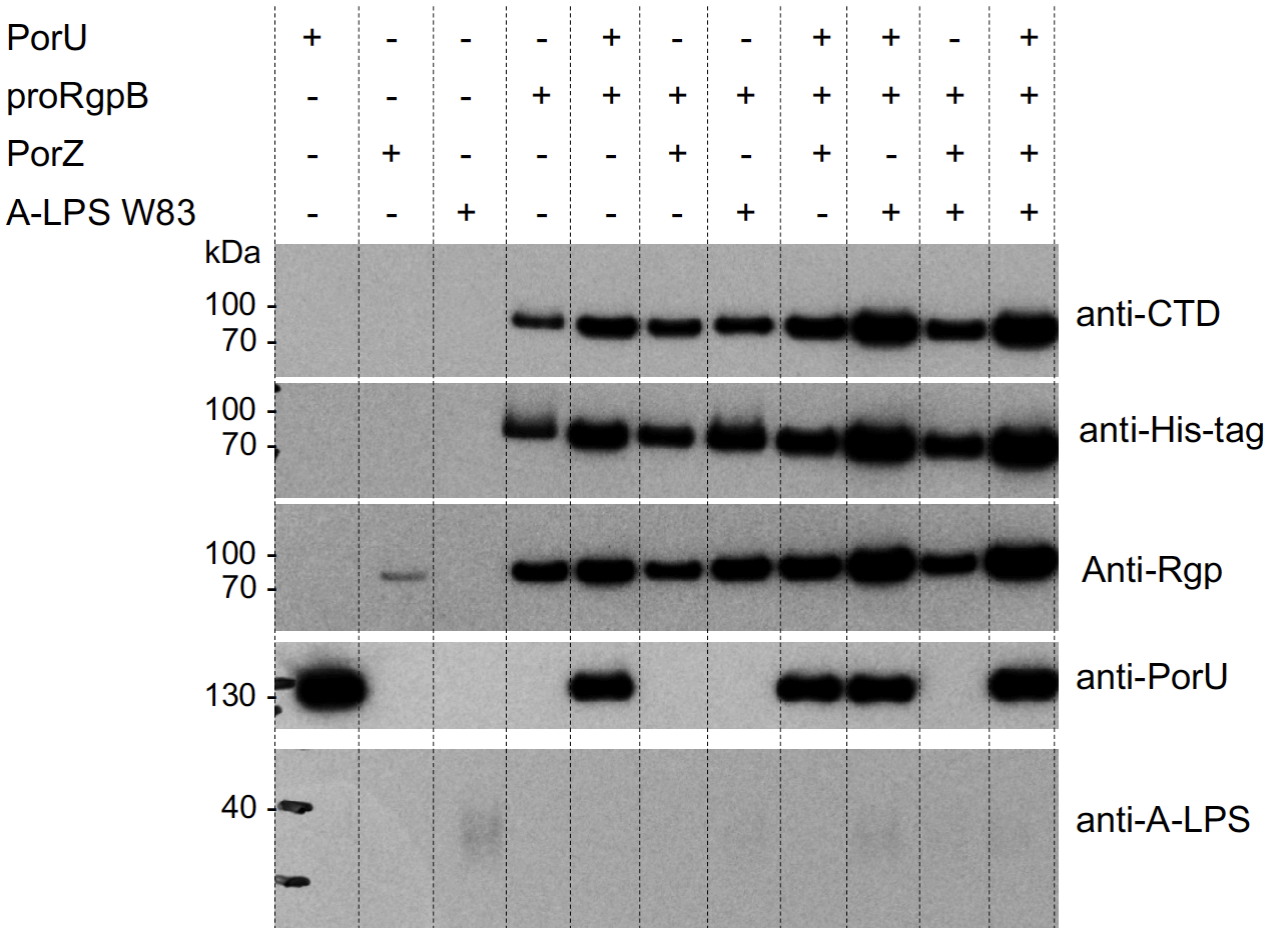

***Suppl. Figure 2* — Analysis of the signal peptidase and transpeptidase functions of rPorU on proRgpB *in vitro*.** Western-blot analysis with polyclonal antibodies against the CTD of proRgpB, polyclonal antibodies against His-tag, polyclonal antibodies against Rgp, and monoclonal antibodies against PorU, depicting the results of incubation of rPorU, proRgpB, and PorZ (all at 1 μM) in the presence of A-LPS isolated from wild-type W83 (A-LPS W83). Freshly isolated monomeric rPorU was pre-activated by incubation in 20 mM L-cysteine for 15 min at 37°C and the reaction was performed in 20 mM Bis-Tris, pH 6.5, 150 mM sodium chloride, 5 mM calcium chloride, and 0.02% sodium azide for 1 h at 37°C. A-LPS W83 was isolated as described (9) and was used at 1×10^5 EU/mL concentration. The proRgpB substrate was not processed under any conditions.

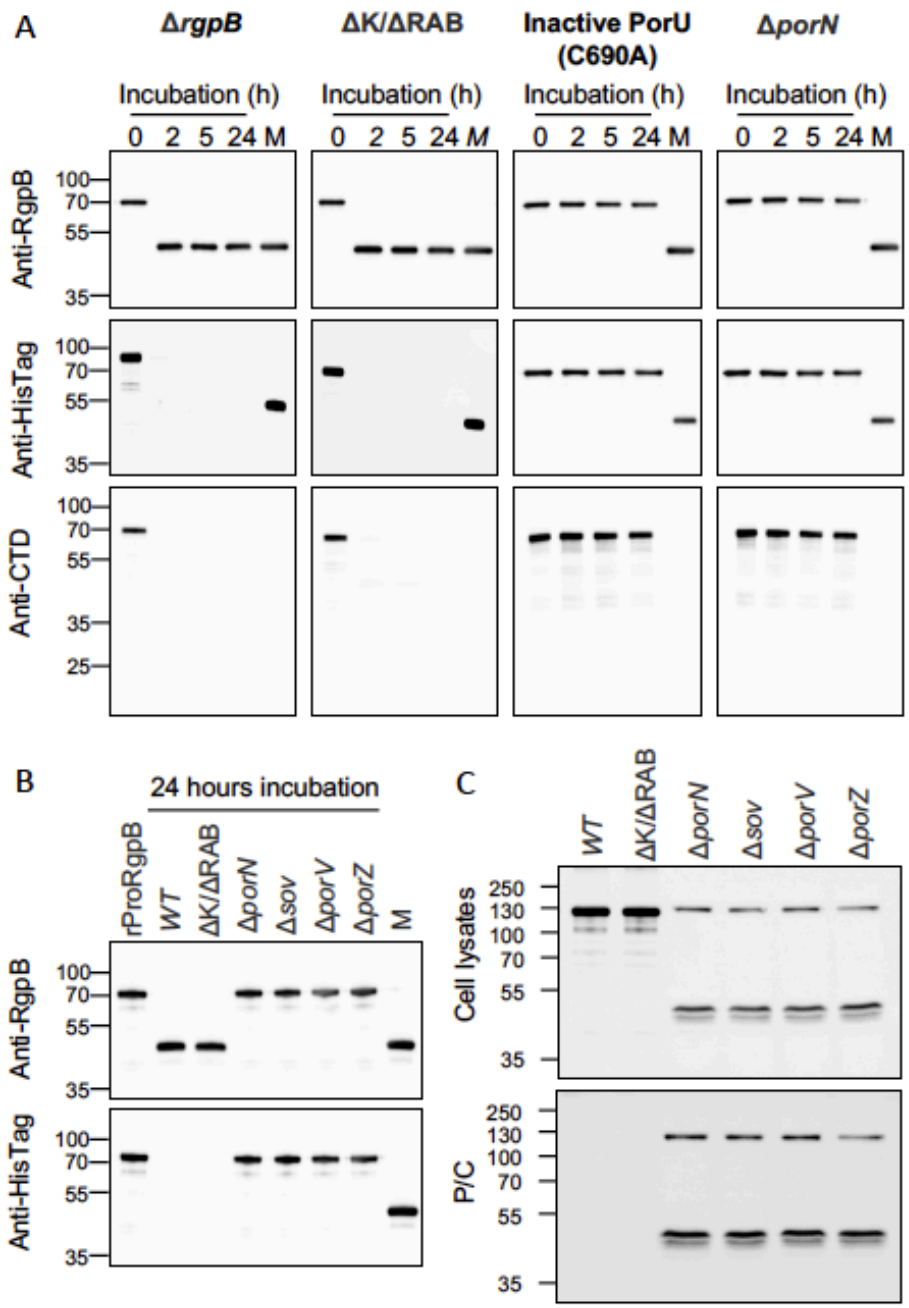

***Suppl. Figure 3* — ProRgpB processing by *P. gingivalis* cell suspension and cell lysates.** ProRgpB^{C449A}-H6 was incubated with *P. gingivalis* cell suspension adjusted to OD_{600}≈0.25 **(A)** or with bacterial cell lysates **(B)** obtained by sonication of wild-type *P. gingivalis* W83 and different mutant strains, including gingipain-null (ΔK/ΔRAB) and T9SS-function-deficient strains (Δ*sov*, Δ*porN*, Δ*porV* and Δ*porZ*). At indicated time points, aliquots were taken and subjected to western-blot analysis using anti-RgpB, anti-HisTag and anti-CTD antibodies. **(C)** Cell lysates (upper panel) and the periplasm/cytoplasm (P/C) fraction (lower panel) were probed for PorU presence by western-blot analysis using a specific anti-PorU antibody. M, RgpB with C-terminal His-tag is shown as marker.

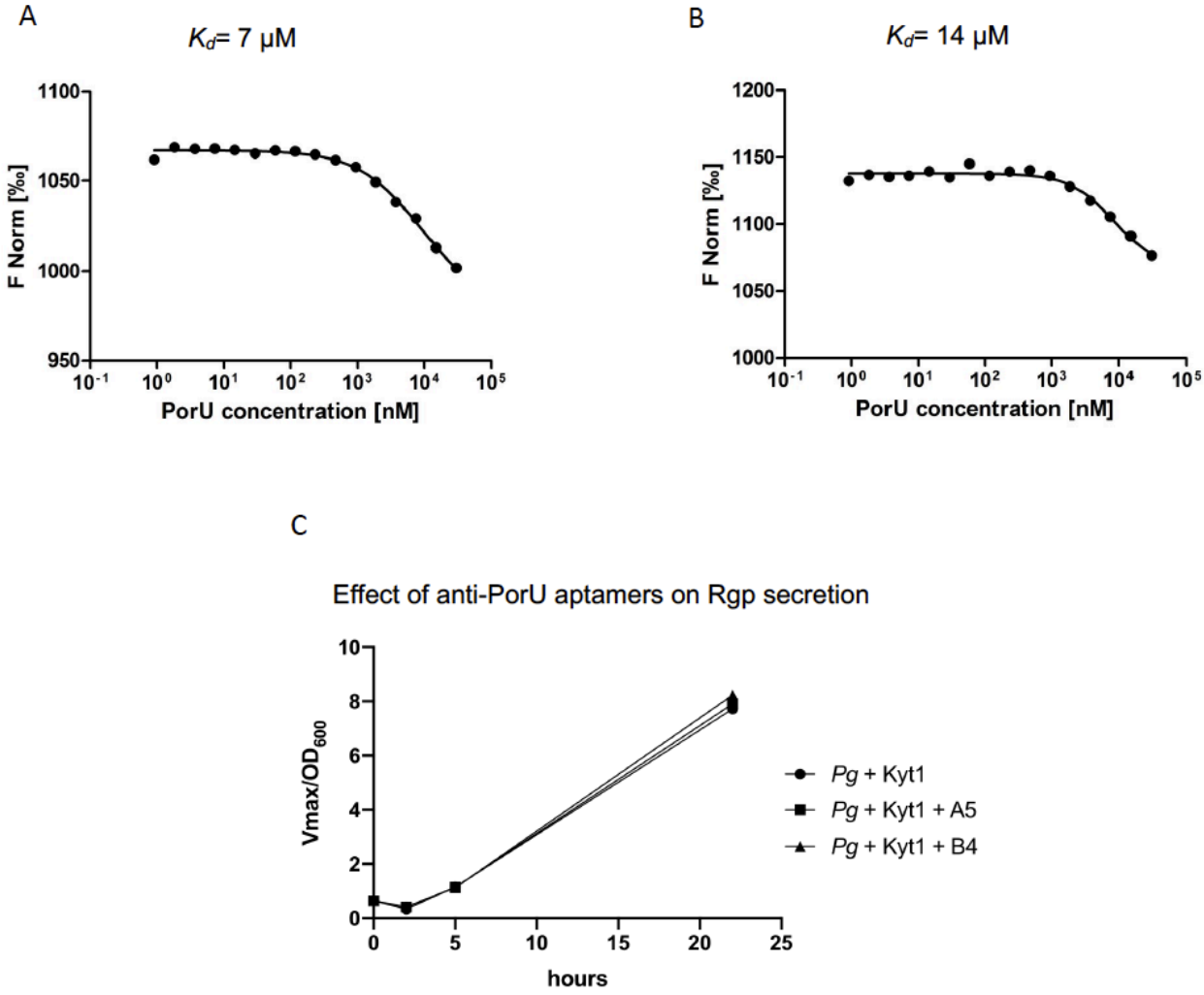

***Suppl. Figure 4* — Aptamers against rPorU do not impair gingipain secretion.** Dissociation constant (K_d) of aptamers A5 (**A**; sequence CATGCTTCCCCAGGGAGATGGTGTGGGTGGGGGGGTGGTGCAGCTG CGGTTGGTGTGTTGGACCCTGGAGGAACATGCGTCGCAAAC) and B4 (**B**; sequence CATGCTTCC CCAGGGAGATGCGGTGGGTTGTTTTGGGTTACTTTGGGGTGGTGGGTATTGAGGACATGCGTCG CAAAC) as determined by microscale thermoforesis. **(C)** To test the effect of these aptamers on gingipain secretion, cultures of *P. gingivalis* at the mid-exponential phase of growth (OD_{600nm}≈0.6) were treated with a Rgp-specific inhibitor to quench existing gingipain activity and aptamers were added (time 0h). At time 0h, 2h, 5h, and 22h Rgp activity was determined using a *p*-nitroanillide substrate. The activity in the culture treated with the inhibitor in the absence of aptamers served as control.

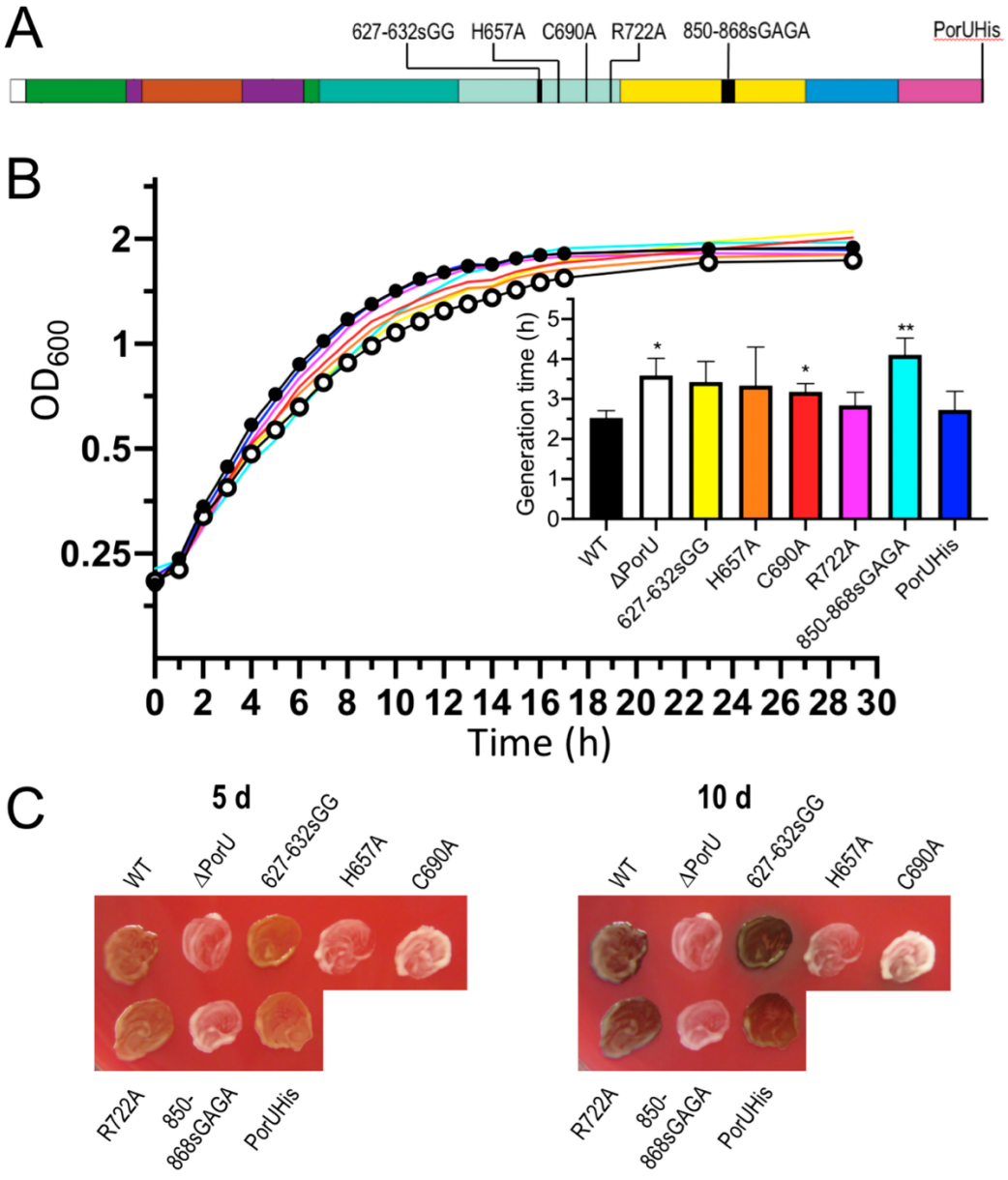

***Suppl. Figure 5* — Growth and pigmentation phenotype of *P. gingivalis* strains used in this study.** (**A**) Scheme depicting the localisation along the sequence of the six PorU variants assayed. **(B)** Growth curve of the six *P. gingivalis* strains coloured as in the inset resulting from optical density measurements (OD_{600}) collected in triplicate over 30 h. The curves of the wild type (WT; full circles) and the deletion mutant ΔPorU (open circles) are included for reference. The generation times g (inset) were calculated with the equation g=0.301/a, where a is the slope of the linear part of the growth curve plotted on a semilogarithmic scale. Experiments were performed in triplicate. Data are presented as means +/- SD and statistical significance was calculated by Student's t-test (* = $p < 0.5$; ** = $p < 0.1$). (**C**) Bacterial strains were plated on blood agar with enriched tryptic soy broth and photographed after anaerobic growth for 5 and 10 days, respectively.

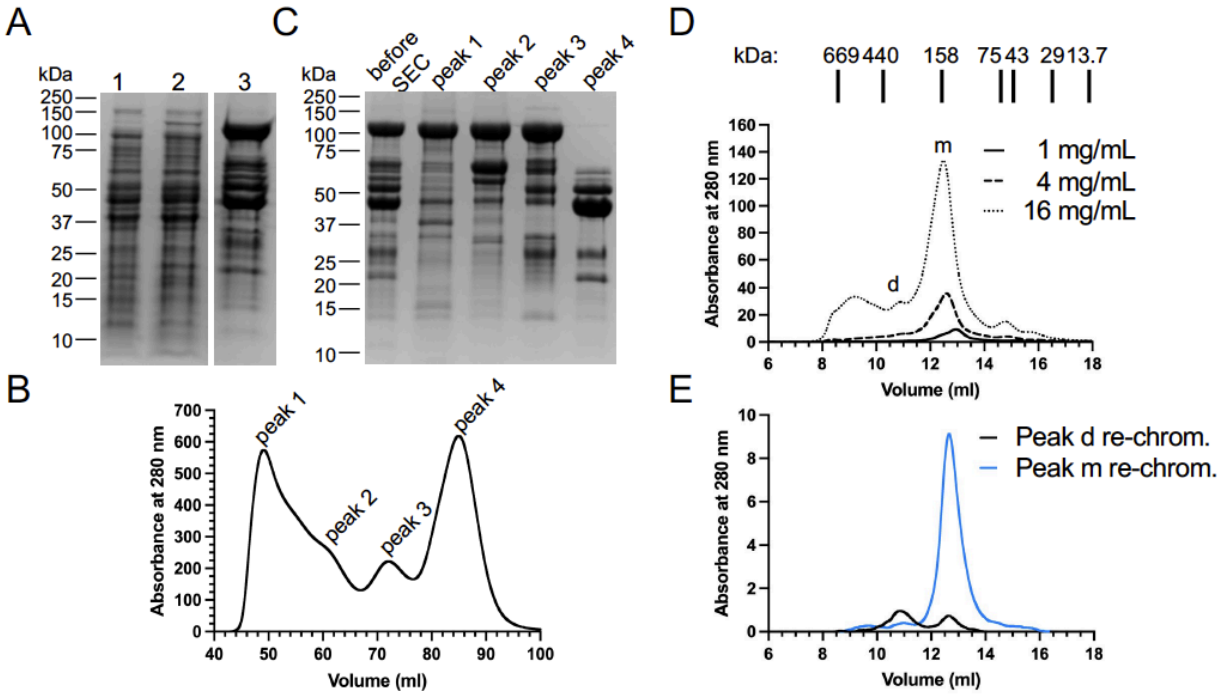

***Suppl. Figure 6* — Expression and purification of PorU$^{850\text{-}868sGAGA}$.** **(A)** Recombinant rPgPorU$^{850\text{-}868sGAGA}$ was expressed in *E. coli* and purified by affinity chromatography. *Lanes 1* and *2*: *E. coli* cells before (1) and after (2) induction of protein expression with IPTG. *Lane 3*: protein eluate from Ni-NTA. **(B)** Monomeric rPgPorU$^{850\text{-}868sGAGA}$ (peak 3) was purified by size-exclusion chromatography (SEC) on a HiLoad 16/60 Superdex 200 pg column (GE Healthcare) equilibrated with 5 mM Tris·HCl pH 8.0, 50 mM sodium chloride, 0.02% sodium azide. **(C)** Fractions corresponding to peaks 1, 2 and 3 of (B) were pooled separately and analysed by SDS-PAGE. **(D)** Monomeric rPgPorU$^{850\text{-}868sGAGA}$ (peak 3) was concentrated to 1-, 4-, and 16 mg/mL and subjected to SEC using a Superdex 200 10/300 GL column (GE Healthcare) equilibrated with PBS pH 7.3, 0.02% sodium azide and calibrated with protein standards (Gel Filtration Calibration Kit, GE Healthcare). **(E)** Fractions corresponding to dimers (d) and monomers (m) were pooled, concentrated and re-chromatographed under the same conditions.

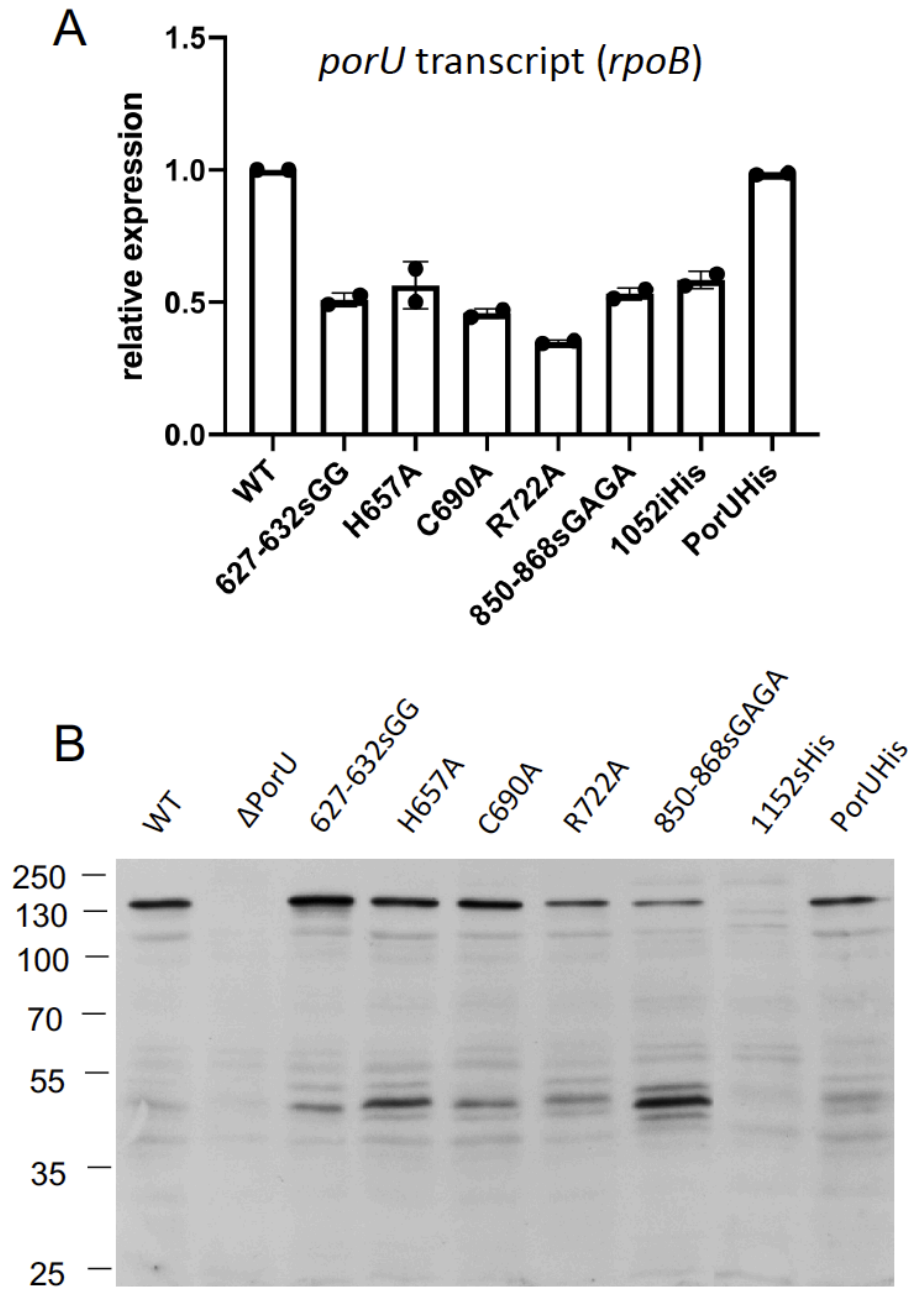

***Suppl. Figure 7* — Levels of *porU* transcript and expressed PorU variants in *P. gingivalis* strains. (A)** Results of qRT-PCR analysis with mRNA isolated from *P. gingivalis* cells collected from a culture grown to OD_{600}≈1.0 (late exponential phase) using a commercial kit (A&A Biotechnology, Poland). Samples were digested with DNase I to remove genomic DNA contaminations, purified again and reverse transcribed with High-Capacity cDNA Reverse Transcription (Applied Biosystems). Quantitative PCR was performed with GoTaq master mix (Promega) with primers: *porU* (n22qPCR_F: CCTCCTTGAGGCTGATCGAC and n22qPCR_R: CCACAGGTGCATTTGCCTTC) and *rpoB* (RpoB For: GGAAGAGAAGACCGTAGCACAA GG and RpoB Rev: GAGTAGGCGAAACGTCCATCAGGT). The reaction was performed in a CFX96 Touch Thermocycler (BioRad). The relative expression levels of the *porU* transcripts was calculated with the *ddCt* method using the *rpoB* gene as a reference. **(B)** Western-blot analysis of *P. gingivalis* cells lysed by sonication. Lysates were adjusted to the same protein concentration, resolved by SDS-PAGE electrophoresis and analysed by western blot using anti-PorU antibodies.

3. SUPPLEMENTARY TABLES

Suppl. Table 1. **Crystallographic data.**

Dataset	**PorU (selenomethionine) Se absorption peak**	**PorU Native**
Space group / protomers per a.u. [a]	$P6_122$ / 2	$P6_122$ / 2
Cell constants a and c (Å)	171.5, 439.3	171.7, 440.4
Wavelength (Å)	0.9793	0.9817
Measurements / unique reflections	1,909,892 / 90,952 [g]	2,159,001 / 56,055
Resolution range (Å) (outermost shell) [b]	88.3–3.50 (3.69–3.50)	88.5–3.35 (3.55–3.35)
Completeness (%)	99.8 (99.7)	100 (100)
R_{merge} [c]	0.197 (2.500)	0.152 (1.899)
R_{meas} [d] / $CC(^1/_2)$ [d]	0.202(2.561)/0.999(0.830)	0.154(1.923)/1.000(0.844)
Average intensity [e]	18.0 (2.2)	22.7 (3.1)
B-Factor (Wilson) (Å^2) / Aver. multiplicity	111.7 / 21.0 (21.3)	107.0 / 38.5 (39.6)
Number of Se atom sites used for phasing	57 (out of 64)	
Resolution range used for refinement (Å)		88.5 – 3.35
Reflections used (test set)		55,218 (836)
Crystallographic R_{factor} (free R_{factor}) [b]		0.202 (0.243)
Non-H protein atoms / solvent molecules / ionic ligands per a.u.		16,378 / 4 / 4 Ca^{2+}
Rmsd from target values of bonds (Å) / angles (°)		0.010 / 1.15
Average B-factor (Å^2)		140.3
Protein contact and geometry analysis [e]		
Residues in favoured Ramachandran regions / outliers / all analysed		1997 (93.0%) / 32 (1.5%) / 2148
Bond-lengths / bond-angles / chirality / planarity ou		0 / 2 / 0 / 4
Side-chain outliers		127 (7.5%)
All-atom clashes / clashscore [f]		42 / 1.3
RSRZ outliers [f] / F_o:F_c correlation [f]		100 (4.6%) / 0.94
PDB access code		6ZA2

[a] Abbreviations: a.u., crystallographic asymmetric unit; RSRZ, real-space R-value Z-score. [b] Values in parenthesis refer to the outermost resolution shell. [c] For definitions, see Table 1 in (30). [d] For definitions, see (31, 32). [e] Average intensity is $\langle I/\sigma(I)\rangle$ of unique reflections after merging according to *Xscale* (9). [f] According to the wwPDB Validation Service (https://wwpdb-validation.wwpdb.org/validservice). [g] Friedel mates were kept separate.

***Suppl. Table 2*. Bacterial strains and plasmids used in this study.**		
Strains	***Description*** *(genotype; resistance)*	***Source***
Escherichia coli DH5α	General cloning host	Thermo Fisher
Escherichia coli BL21 (DE3)	Expression of PorU protein variants	Millipore
Porphyromonas gingivalis		
WT	Wild-type W83 strains	
ΔPorU	*porU::ermF;* Em^r	(33)
PorUHis	*porU1158ins8His, ermF;* Em^r	This study
PorU-627-632sGG	*porU 627-632::GG, 1158ins8His, ermF;* Em^r	This study
PorU-H657A	*porU H657A,1158ins8His, ermF;* Em^r	This study
PorU-C690A	*porU C690A,1158ins8His, ermF;* Em^r	This study
PorU-R722A	*porUR722A,1158ins8His, ermF;* Em^r	This study
PorU-850-868sGAGA	*porU 850-868::GAGA, 1158ins8His, ermF;* Em^r	This study
Plasmids	***Relevant features***	
pPorU-E	Master plasmid for PorU modification, derivative of pUC19	(33)
pET-Duet-1-PorU	Plasmid for PorU purification, derivative of pET-Duet-1	(34)
pPorUHis (1158iHis)	Plasmid for 1158iHis mutagenesis in PorU, derivative of pPorU-E	This study
pPorUHis_627-632sGG	Plasmid for 627-632sGG mutagenesis in PorU, derivative of pPorUHis	This study
pPorUHis_H657A	Plasmid for 627-632sGG mutagenesis in PorU, derivative of pPorUHis	This study
pPorUHis_C690A	Plasmid for 627-632sGG mutagenesis in PorU, derivative of pPorUHis	This study
pPorUHis_R722A	Plasmid for 627-632sGG mutagenesis in PorU, derivative of pPorUHis	This study
pPorUHis_850-868sGAGA	Plasmid for 627-632sGG mutagenesis in PorU, derivative of pPorUHis	This study

***Suppl. Table 3*. List of primers (5' → 3') used in this study.**	
pET-Duet-1-PorU	
PG26-F	TGGACTGCAGCAACGAGCTATGGGGAAGACGG
PG26-R	CTGGCTCGAGCTATTGTCCTACCACGATCATTTTCTTGG
PorUHis (1158iHis)	
P22i6h_Fs	TAGCCTCTAGAATAGCTTCCGC
P22i6h_Ft	CACCATCACCATCACCATTAGCCTCTAGAATAGCTTCCGC
P22i6h_Rs	TTGTCCTACCACGATCATTTTC
P22i6h_Rt	ATGGTGATGGTGATGGTGTTGTCCTACCACGATCATTTTC
pPorUHis_627-632sGG	
627GGFt	ATATCCGCATGTCGGTGGCAGCATTCCGGGTGCAAAGA
627GGFs	CAGCATTCCGGGTGCAAAGA
627GGRt	CCACCGACATGCGGATATACGTCCTGAAAGGCGCGTAC
627GGRs	ACGTCCTGAAAGGCGCGTAC
pPorUHis_H657A	
newH634AF	*GGCGGTCCTGCCGGATGGGCT
newH634AR	*AGCACCAGCATAATTAAGCAGGATAATACCC
pPorUHis_C690A	
22C667AFt	TTACTGCCACGGCCGACTTTGCCAACTATGACAGTCAGA
22C667ARt	AGTCGGCCGTGGCAGTAATCCAAATGGGCATATGCTTAT
P22C2162AFs	TTGCCAACTATGACAGTCAGA
P22C2162ARs	TCCAAATGGGCATATGCTTAT
pPorUHis_R722A	
porUR722AFs	GCAGAATGAGAAGATCAATGGT
porUR722ARs	GTAGTCGAGAACATGATCGGA
porUR722AFt	GGCTGTCGTTTACAATACGCAGAATGAGAAGATCAATGGT
porUR722ARt	GTATTGTAAACGACAGCCGTAGTCGAGAACATGATCGGA
pPorUHis_850-868sGAGA	
porU2G2AFt	GGAGCTGGTGCACCTAACGTGATGTATGCCGGTATTGCC
porU2G2ARt	GTTAGGTGCACCAGCTCCCTTTCTGCCATCGAAGACGG
* phosphorylation.	

4. SUPPLEMENTARY REFERENCES

1. J. Chiu, P. E. March, R. Lee, D. Tillett, Site-directed, ligase-independent mutagenesis (SLIM): a single-tube methodology approaching 100% efficiency in 4h. *Nucleic Acids Res.* **32**, e174 (2004).
2. D. G. Gibson *et al.*, Enzymatic assembly of DNA molecules up to several hundred kilobases. *Nat. Methods* **6**, 343-345 (2009).
3. M. Bélanger, P. Rodrigues, A. Progulske-Fox, Genetic manipulation of *Porphyromonas gingivalis*. *Curr. Protoc. Microbiol.* **Chapter 13**, Unit13C 12 (2007).
4. F. Veillard *et al.*, Purification and characterisation of recombinant His-tagged RgpB gingipain from *Porphymonas gingivalis*. *Biol. Chem.* **396**, 377-384 (2015).
5. K. N. Hosn, M. M. Jefferson, C. Leding, S. Shokouh-Amiri, E. L. Thomas, Inhibitors of bacterial protease enzymes for periodontal therapy. *Clin. Exp. Dent. Res.* **1**, 18-25 (2015).
6. L. Marino-Puertas, L. Del Amo-Maestro, M. Taules, F. X. Gomis-Rüth, T. Goulas, Recombinant production of human α_2-macroglobulin variants and interaction studies with recombinant G-related α_2-macroglobulin binding protein and latent transforming growth factor-β_2. *Sci. Rep.* **9**, 9186 (2019).
7. S. R. Mendes *et al.*, Analysis of the inhibiting activity of reversion-inducing cysteine-rich protein with Kazal motifs (RECK) on matrix metalloproteinases. *Sci. Rep.* **10**, 6317 (2020).
8. B. W. Matthews, Solvent content of protein crystals. *J. Mol. Biol.* **33**, 491-497 (1968).
9. W. Kabsch, XDS. *Acta Crystallogr. sect. D* **66**, 125-132 (2010).
10. P. D. Adams *et al.*, PHENIX: a comprehensive Python-based system for macromolecular structure solution. *Acta Crystallogr. sect. D* **66**, 213-221 (2010).
11. M. D. Winn *et al.*, Overview of the CCP4 suite and current developments. *Acta Crystallogr. sect. D* **67**, 235-242 (2011).
12. G. M. Sheldrick, Experimental phasing with SHELXC/D/E: combining chain tracing with density modification. *Acta Crystallogr. sect. D* **66**, 479-485 (2010).
13. G. M. Sheldrick, The *SHELX* approach to experimental phasing of macromolecules. *Acta Crystallogr. sect. A* **67**, C13 (2011).
14. T. C. Terwilliger *et al.*, Decision-making in structure solution using Bayesian estimates of map quality: the PHENIX AutoSol wizard. *Acta Crystallogr. sect. D* **65**, 582-601 (2009).
15. T. C. Terwilliger *et al.*, Iterative model building, structure refinement and density modification with the PHENIX AutoBuild wizard. *Acta Crystallogr. sect. D* **64**, 61-69 (2008).
16. A. Casañal, B. Lohkamp, P. Emsley, Current developments in *Coot* for macromolecular model building of electron cryo-microscopy and crystallographic data. *Protein Sci.* **29**, 1069-1078 (2020).
17. D. Liebschner *et al.*, Macromolecular structure determination using X-rays, neutrons and electrons: recent developments in *Phenix*. *Acta Crystallogr. sect. D* **75**, 861-877 (2019).
18. O. S. Smart *et al.*, Exploiting structure similarity in refinement: automated NCS and target-structure restraints in BUSTER. *Acta Crystallogr. sect. D* **68**, 368-380 (2012).
19. M. Källberg *et al.*, Template-based protein structure modeling using the RaptorX web server. *Nat. Protoc.* **7**, 1511-1522 (2012).
20. A. Eichinger *et al.*, Crystal structure of gingipain R: an Arg-specific bacterial cysteine proteinase with a caspase-like fold. *EMBO J.* **18**, 5453-5462 (1999).
21. I. de Diego *et al.*, *Porphyromonas gingivalis* virulence factor gingipain RgpB shows a unique zymogenic mechanism for cysteine peptidases. *J. Biol. Chem.* **288**, 14287-14296 (2013).
22. B. Webb, A. Šali, Protein structure modeling with MODELLER. *Methods Mol. Biol.* **1654**, 39-54 (2017).
23. T. Guevara *et al.*, Structural determinants of inhibition of *Porphyromonas gingivalis* gingipain K by KYT-36, a potent, selective, and bioavailable peptidase inhibitor. *Sci. Rep.* **9**, 4935 (2019).
24. V. B. Chen *et al.*, MolProbity: all-atom structure validation for macromolecular crystallography. *Acta Crystallogr. sect. D* **66**, 12-21 (2010).
25. L. Holm, P. Rosenström, Dali server: conservation mapping in 3D. *Nucleic Acids Res.* **38**, W545-W549 (2010).
26. E. Krissinel, K. Henrick, Secondary-structure matching (SSM), a new tool for fast protein structure alignment in three dimensions. *Acta Crystallogr. sect. D* **60**, 2256-2268 (2004).
27. E. F. Pettersen *et al.*, UCSF Chimera - A visualization system for exploratory research and analysis. *J. Comput. Chem.* **25**, 1605-1612 (2004).

28. A. Drozdetskiy, C. Cole, J. Procter, G. J. Barton, JPred4: a protein secondary structure prediction server. *Nucleic Acids Res.* **43**, W389-W394 (2015).
29. E. Krissinel, K. Henrick, Inference of macromolecular assemblies from crystalline state. *J. Mol. Biol.* **372**, 774-797 (2007).
30. R. García-Castellanos *et al.*, Three-dimensional structure of MecI : Molecular basis for transcriptional regulation of staphylococcal methicillin resistance. *J. Biol. Chem.* **278**, 39897-39905 (2003).
31. M. S. Weiss, Global indicators of X-ray quality. *J. Appl. Cryst.* **34**, 130-135 (2001).
32. P. A. Karplus, K. Diederichs, Linking crystallographic model and data quality. *Science* **336**, 1030-1033 (2012).
33. A. M. Lasica *et al.*, Structural and functional probing of PorZ, an essential bacterial surface component of the type-IX secretion system of human oral-microbiomic *Porphyromonas gingivalis*. *Sci. Rep.* **6**, 37708 (2016).
34. M. Madej *et al.*, PorZ, an essential component of the type IX secretion system of *Porphyromonas gingivalis*, delivers anionic lipopolysaccharide to the PorU sortase for transpeptidase processing of T9SS cargo proteins. *mBio* **12**, e02262-02220 (2021).